Multi-Frequency NMR and TGA Characterization of TOC in Shales

B.C. Anger[a]*, M. Rydzy[a], N.P. Ramskill[b], S. Hertel[a], A.J. Sederman[b],
M.D. Mantle[b], L.F. Gladden[b], M. Appel[a]
[a]Shell Technology Center Houston, 3333 Highway 6 South, Houston, TX USA
[b]Department of Chemical Engineering and Biotechnology, University of Cambridge,
Cambridge CB2 3RA, UK
(*Corresponding Author's email: benjamin.anger@shell.com)

This paper was prepared for presentation at the International Symposium of the Society of Core Analysts held in Snowmass, Colorado, USA, 21-26 August 2016

ABSTRACT

The production of unconventional shale assets depends on an understanding of pore structure, fluid content and distribution within the reservoir rock. The nanometer scale pores and range of hydrocarbon types (mobile vs. immobile hydrocarbons) present in shale reservoirs lead to difficulty in using conventional petrophysical measurements to produce quantitative values for important parameters such as porosity, fluid content or saturation. Many existing techniques can be used to characterize these materials, but it can be useful to combine multiple standard measurements to provide a more quantitative understanding of rock properties. T_1-T_2 NMR relaxation maps can provide insight into the fluids present in the shales, and measurements of the total organic content (TOC) provide an estimate of the amount of organic material. Since the NMR signal in shales is largely due to the hydrocarbons in place, it is probable that magnetic resonance should provide a direct probe of the amount and type of hydrocarbon types in a shale sample. Further clarification can be provided by the addition of thermal analysis methods combined with mass spectroscopy.

In this work, we present experimental results showing not only a direct correlation between TOC and T_1/T_2 ratio as measured by 2D NMR, but also a frequency dependence of this relationship. We further correlate these results with compositional data provided by thermogravimetric analysis with mass spectroscopy (TGA-MS). Our measurements cover several different shale types and span a wide range of TOC. 2D NMR spectra were obtained at multiple frequencies on crushed shale samples that were exposed to the key temperatures indicated in the TGA results. The results helped to correlate compositional changes to regions of the 2D relaxation maps, potentially providing a method for determining the amount of mobile and immobile hydrocarbons that constitute the total organic carbon content in shale.

INTRODUCTION

The characterization of organic shales continues to be a challenge in the petroleum industry. Many techniques used for the characterization of conventional reservoir rocks cannot reliably be used to determine the petrophysical properties of shales and other unconventional source rocks. Even the determination of basic properties such as porosity and permeability can be complicated by the additional physical interactions in these materials due to the presence of hydrogen-bearing organic solids that are not present in conventional formations, e.g. sandstones and carbonates. A continuing challenge is the differentiation between the fluid types present in organic shales. Standard one-dimensional nuclear magnetic resonance measurements of the transverse relaxation time T_2 are unable to separate the effects of water and hydrocarbons in shales [1-2] since signals from water, hydrocarbons and organic matter overlap in T_2 spectra. Multidimensional NMR measurements offer deeper insights into the contributions of the various species present in organic reservoir rocks. While there is overlap of the NMR signal from the various components in the T_2 dimension, extension of experiments to include T_1 [2-9] or diffusion [10] effects provides an additional resolution that allows for potential signal source differentiation. The ratio of T_1/T_2 has long been viewed as an important means for the characterization of rock/fluid interactions [5-6, 11-13]. The addition of multi-frequency studies and fast field cycling (FFC) NMR [13-15] has recently provided another tool for the description of fluid physics in organic shales. Birdwell and Washburn also recently showed that T_1-T_2 maps can be used for understanding geochemical data [16]. Robust models for T_1-T_2 fluid mapping are now emerging [9]. Further efforts to understand multidimensional NMR relaxation spectra have enlisted thermogravimetric analysis and retort methods to correlate changes in sample mass to NMR response [17-18].

In this work, we present experimental evidence of a dependence of the T_1/T_2 ratio on both frequency and TOC in multiple shale samples. We further measured the mass changes of a series of shale samples during a multi-step heating process. Sample mass changes were compared to changes in both the 1D and 2D NMR relaxation spectra and analyzed in light of TGA-MS data acquired on the same sample sets.

EXPERIMENTAL

The samples used in this work were sourced from two gas shale formations, referred to in this work as shales A and B. Prior to these experiments, the TOC (WT%) had been measured by LECO for each sample set, and ranged from ~1% to ~10% by weight. Information on the shale sample sets can be found in table 1. Both sample sets were in the as-received condition.

Each sample set was subjected to the following experimental techniques: NMR, TGA-MS and oven drying under a He atmosphere.
- **Sample Preparation:** In order to facilitate drying and TGA-MS measurements, all samples were crushed by hand to 45 mesh (0.354 mm).

- **Oven Drying:** Based on initial TGA-MS results, the crushed shale A samples were baked for 48 hours under a He purge at 120 °C and 220 °C. The final temperature was chosen to remove both water and liquid hydrocarbons while minimizing the conversion of solid hydrocarbons to liquid form [19].
- **NMR:** 1D (T_1 and T_2) and 2D (T_1-T_2) relaxation spectra of both sample sets were acquired at 2.3 MHz, 12.7 MHz and 23.3 MHz on Oxford Instruments spectrometers with echo times, TE = 0.134 ms, 0.164 ms and 0.132 ms respectively. The 2D T_1-T_2 inversion recovery delay lists were logarithmically spaced with 30-50 entries and varied from 10 µs to 5.6 s. NMR results were processed using in-house 1D and 2D inverse Laplace transform algorithms. Shale A as-received NMR acquisitions were performed on secondary set of material, and all quantitative measurements on shale A presented here are normalized by sample mass to allow for direct comparison.
- **TGA-MS:** TGA-MS measurements were performed on both sample sets with a PerkinElmer Pyris 1 TGA coupled to a Clarus SQ8 MS mass spectrometer. The TGA measures changes in sample mass as a function of temperature during heating while the MS determines the composition of the material evaporating from the sample. Approximately 35-65 mg of crushed material were heated from room temperature to 850 °C at a rate of 10 °C/minute with ten minute holds at 50 °C and 850 °C.

Shale A	TOC (WT%)	Shale B	TOC (WT%)
A1	1.43	B1	0.12
A2	2.15	B2	1.22
A3	2.59	B3	2.42
A4	3.15	B4	3.01
A5	3.42	B5	4.25
A6	4.15	B6	6.65
A7	6.75	B7	7.08
A8	10.66	B8	9.09
		B9	9.35
		B10	10.12

Table 1: TOC (WT%) values for shales A and B.

FREQUENCY AND TOC DEPENDENCE OF T_1/T_2 RATIO

Standard NMR relaxation models in porous media are difficult to apply in organic shales due to nanometer-scale pore sizes and additional relaxation mechanisms active caused by the presence of solid organic materials. The relaxation times T_1 and T_2 of pseudo-solid materials were described by Bloembergen, Purcell and Pound [20-21] in relation to the correlation time τ of the dipolar interactions:

$$\frac{1}{T_1} = 2C\left[\frac{2\tau}{1+\omega^2\tau^2} + \frac{8\tau}{1+4\omega^2\tau^2}\right] \tag{1}$$

$$\frac{1}{T_2} = C\left[6\tau + \frac{10\tau}{1+\omega^2\tau^2} + \frac{4\tau}{1+4\omega^2\tau^2}\right] \tag{2}$$

where C is a constant and ω is the Larmor frequency. In the limit of fast diffusion ($\omega\tau \ll 1$), typically obtained for the isotropic tumbling of small, mobile molecules, $T_1 = T_2$. This is typically the case for mobile fluids in the large pores of conventional reservoir rocks. In the case, however, of organic shales, the small pores and large, relatively immobile hydrocarbon molecules, the fast diffusion limit is no longer relevant. For these materials, the ratio T_1/T_2 becomes larger than 1, and, in the limit of $\omega\tau \gg 1$, T_1/T_2 becomes proportional to $\omega^2\tau^2$. A large T_1/T_2 ratio is indicative of the presence of hydrocarbons and solid organics in shale materials [9].

In this work, 1D and 2D NMR measurements were made on shales A and B at 2 MHz, 12 MHz and 23 MHz. A representative set of T_1-T_2 maps for shale A7 is found in figure 1. In these results, two peaks are typically observed: the peak at shorter T_1 values corresponds to mobile and clay bound water while the higher T_1 peak likely corresponds to mobile hydrocarbons. To guide the eye, dashed lines are plotted for $T_1/T_2 = 1$ as well as through the higher T_1/T_2 peak. The logarithmic scale in the T_1-T_2 maps allows for a large variation in the estimated T_1/T_2 ratio for a peak when picking by eye the best fit line passing through the center of the peak. In order to minimize bias, these values were determined with a 2D peak finding routine in Matlab [22] that detects all local maxima. However, even with this automation, it can be difficult to determine the best value for T_1/T_2 due to the often extended and asymmetric nature of the peaks in question. The best T_1/T_2 ratio was then determined for the desired peak. The resulting T_1/T_2 ratios for the high ratio peak are plotted against NMR frequency for a representative selection of shale A samples in figure 2. Similar behavior was observed in the shale B samples.
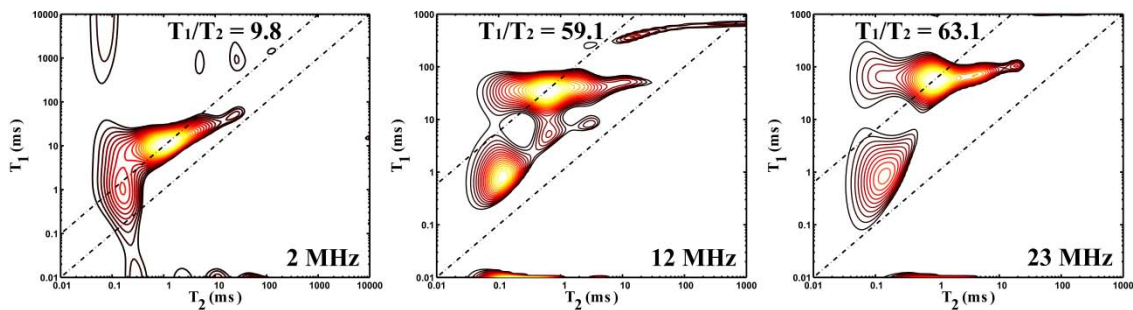

Figure 1: Frequency dependence of T_1/T_2 in sample A7. The lower diagonal lines correspond to $T_1/T_2 = 1$.
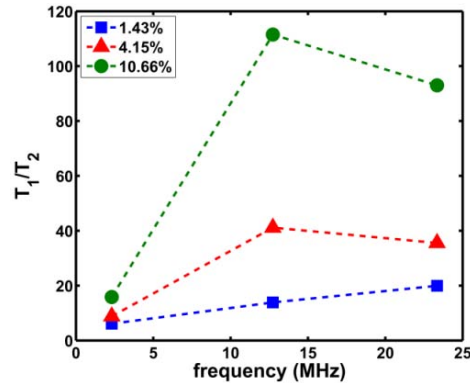
Figure 2: Dependence of T_1/T_2 ratio on NMR frequency a representative selection of shale A samples.

As expected, a general dependence of the T_1/T_2 ratio on frequency was observed for both shale A and shale B. However, the predicted $\omega\tau_2$ dependence is not seen, and in many cases T_1/T_2 is higher at 12 MHz than at 23 MHz. No assumptions have been made regarding the relevant correlation times, and further information about the composition of the organic matter present in the samples is likely required to explain this discrepancy. Also, the inexact nature of determining the best value for T_1/T_2 has the potential to introduce large uncertainties which could obscure the presence of any frequency dependence. Further work is needed to determine a robust and accurate method for the quantitative analysis of T_1-T_2 maps.

Figure 3 shows the dependence of T_1/T_2 on TOC for both sample sets. In both cases, a clear increase in T_1/T_2 is observed for the larger TOC values with a more pronounced effect seen at 12 MHz and 23 MHz. While not as clearly evident in the shale B data, there appears to exist a threshold or transition at roughly 4-5% TOC by weight. Above this value, T_1/T_2 increases rapidly for increasing TOC while below the threshold the spread in T_1/T_2 values is nearly constant for all frequencies and TOCs.
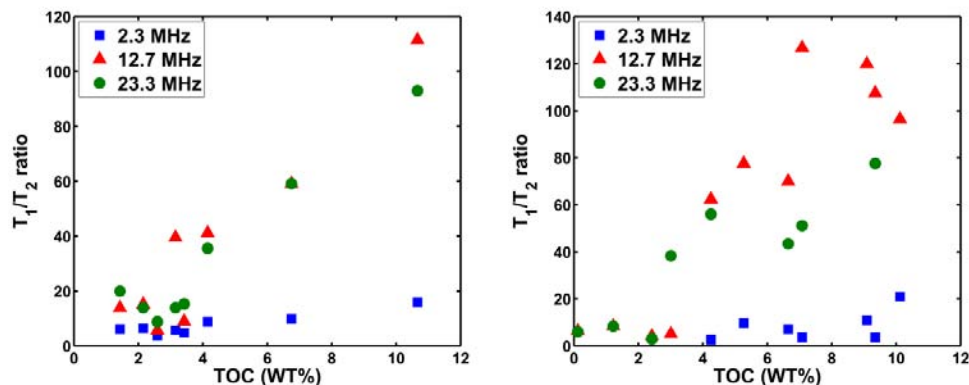

Figure 3: Dependence of T_1/T_2 ratio on TOC (WT%) a) shale A and b) shale b sample sets.

In order to explore this behavior more thoroughly, the variation in the 1D NMR relaxation spectra was explored. In general, the frequency dependence of T_1 is stronger

than that of T_2, and this carries through to the value of T_1/T_2. Figure 4 shows a representative set of 1D projections of T_1, T_2 and T_1/T_2 data for sample A6 from the T_1-T_2 map. The T_1 data shows more than an order of magnitude difference between 2 MHz and 23 MHz while the T_2 spectra are nearly identical at all frequencies. This general behavior was observed for all shale A samples. The weak dependence of T_2 with frequency is potentially an important result for core-to-log integration of laboratory NMR data. Downhole logging tools measure T_2 over a range of frequencies from ~500 kHz to several MHz while laboratory core T_2 measurements are typically made at 2 MHz. In the case of organic shales, even simple T_2 acquisitions can require several hours. The data in figure 4 suggests that laboratory T_2 measurements on shales can safely be made at higher fields, potentially offering a significant decrease in acquisition time as the NMR signal's dependence on frequency scales as $\omega^{3/2}$, leading to a potential signal increase of more than a factor of 30 when measurements are made at 23.3 MHz instead of 2.3 MHz. However, care must be taken when T_1 or T_1-T_2 measurements are performed at higher fields as the much stronger dependence of T_1 on frequency could affect results.
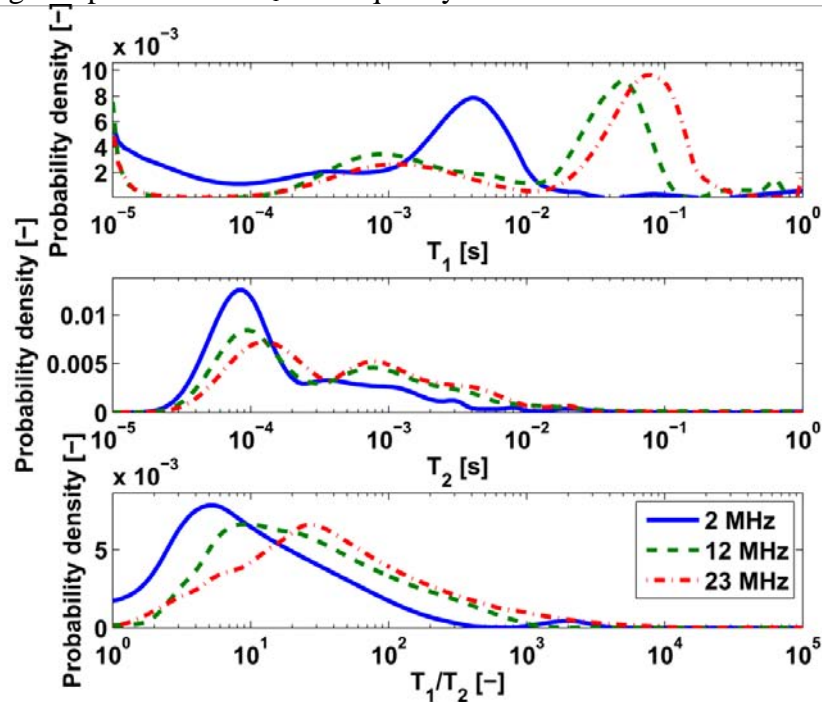

Figure 4: T_1, T_2 and T_1/T_2 projections of T_1-T_2 map for as-received sample A6.

The dependence of T_1 on frequency is also observed in shale A for regions of high and low T_1/T_2 on T_1-T_2 maps. Figure 5 shows the T_1 behavior in two regions for all shale A samples. Plot A shows the maximum T_1 value in the region <1 ms for 2 MHz relaxation data and <10 ms for 12 MHz and 23 MHz data while plot B shows the maximum T_1 value at times >1 ms for 2 MHz data and >10 ms for 12 MHz and 23 MHz data. The error bars are given by the standard deviation across all samples.
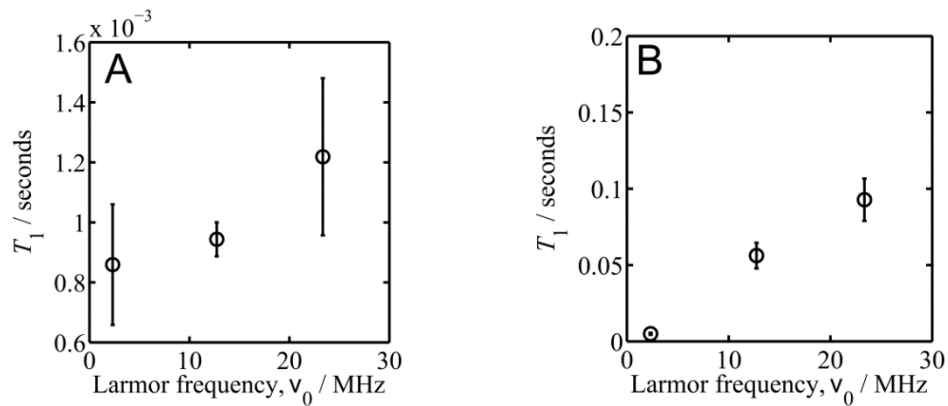
Figure 5: Frequency dependence of T_1 for long and short T_1 regions in as-received shale A for a) T_1<1 ms at 2 MHz and <10 ms at 12 and 23 MHz and b) T_1>1ms at 2 MHz and >10 ms at 12 and 23 MHz.

THERMOGRAVIMETRIC ANALYSIS AND OVEN DRYING

Several groups have reported on efforts to correlate the NMR response of organic shales to the composition and volume of pore fluids and organics present in reservoir materials [15, 17-18]. In this work, we report the results of TGA-MS analysis of shale A as well as changes in the mass of each sample after oven baking under a He purge. TGA data for a subset of shale A samples can be found in figure 6.
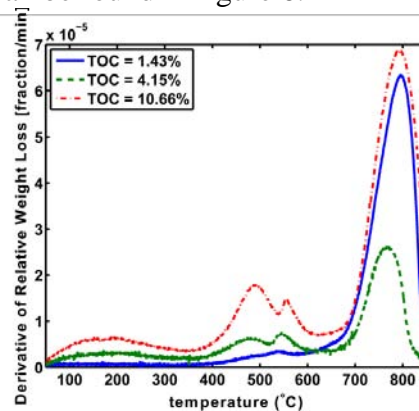

Figure 6: TGA results for samples A1, A6 and A8.

The TGA data show several peaks. A broad peak is found between 50 °C and 350 °C which indicates the evaporation of free water and mobile hydrocarbons. Above 350 °C, structural water and kerogen are produced [23-24]. The large peak at 750 °C is due to chemical changes in the rock matrix and clays. This interpretation is supported by the mass spectroscopy data for water (M/Z = 18) and butyl, and indicator of hydrocarbons with M/Z = 57, which can be found in figure 7. Our mass spectroscopy results show the evolution of both water and mobile hydrocarbons below 350 °C. It is possible to use mass spectroscopy data to independently determine the changes in relative saturation levels of water and hydrocarbons [15]. The combination of TGA and mass spectroscopy also provided insight into the type of organic matter present in the shale A samples. For TOC values less than 5%, the organic material present in the sample was predominantly

immobile while more mobile hydrocarbons were present in samples for which TOC > 5%.
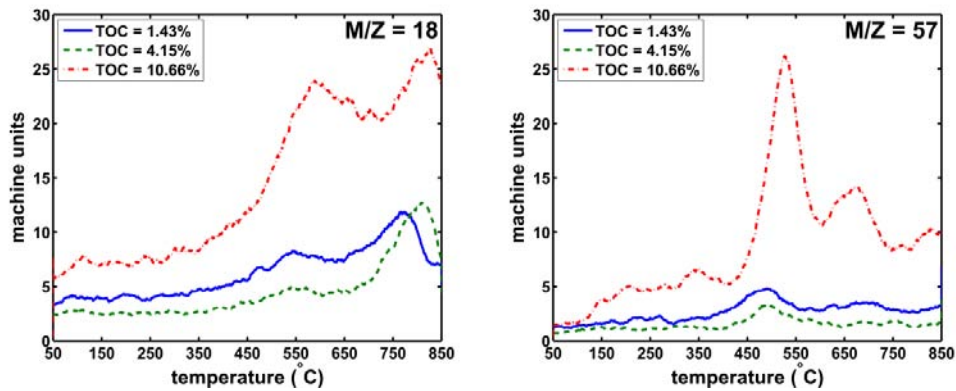

Figure 7: Shale A mass spectroscopy results for a) water and b) hydrocarbon indicator butyl.

TGA data for shale B samples also provided insights into sample mineralogy. Figure 8 shows the TGA results for three shale B samples containing a) mainly immobile hydrocarbons (B8), b) mainly clay (B4) and c) an equal mix of hydrocarbons and clay (B3). This variation indicates that the environment for the bound water could vary strongly between samples.
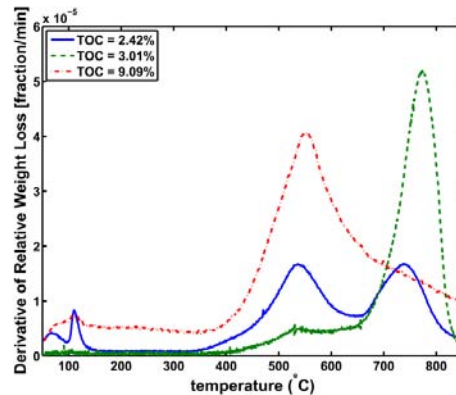

Figure 8: TGA results for shales B3 (TOC=2.42%), B4 (TOC=3.01%) and B8 (TOC=9.09%).

One goal of this work was to correlate changes in 2D T_1-T_2 maps of organic shales to gravimetric changes after baking. Guided by the TGA-MS data, shale A samples were baked for 48 hours under a He purge at 120 °C and 220 °C after which T_2 and T_1-T_2 measurements were made. A series of T_1-T_2 maps for single shale A sample normalized to the as-received sample data is found in figure 9.
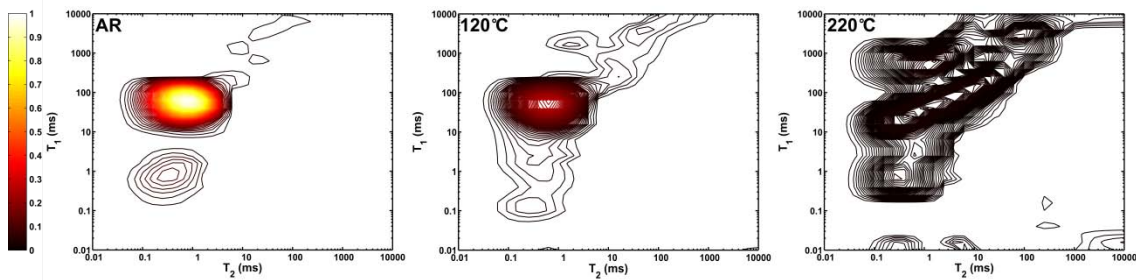
Figure 9: T_1-T_2 maps for a) as-received shale A8, after baking at b) 120 °C and c) 220 °C. The intensity scale has been normalized to the as-received data.

A clear decrease in signal intensity is observed in all areas of the map. Plots of the change in integrated NMR volume for both the high T_1/T_2 ratio peak as well as the lower T_1/T_2 ratio peak were made to determine if it is possible to independently track changes in pore fluids. Normalized results are shown in figure 10 for samples A1, A6 and A8. This figure shows that the integrated NMR volumes of both high and low T_1/T_2 ratio peaks appear to decrease at the same rate, indicating that, for the shale A sample set, both water and mobile hydrocarbons are leaving the sample during baking at 120 °C and 220 °C.
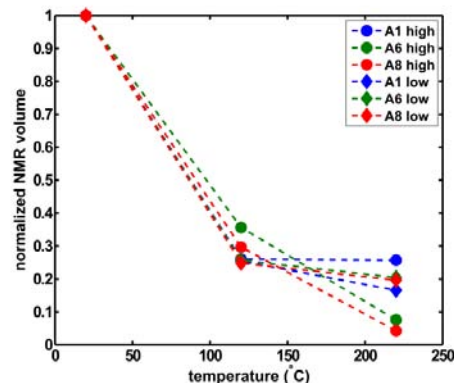

Figure 10: Comparison of changes in high T_1/T_2 and low T_1/T_2 peaks for samples A1, A6 and A8. Dotted lines are added to guide the eye.

Changes in sample mass after each baking step were tracked and compared to changes in the integrated NMR volume. In calculating the NMR volume, no assumptions were made regarding the relative volumes of hydrocarbons and water, and a hydrogen index of 1 was used. As seen in figure 11, the two quantities appear to be well correlated. Ideally, the trendline should extend through the origin. More precise integrations of our mass spectroscopy data will allow more precise determination of the relative masses of water and hydrocarbons evolved during heating which will allow for a more realistic slope and intercept of the best fit line through the data. Efforts are currently underway to acquire such data.
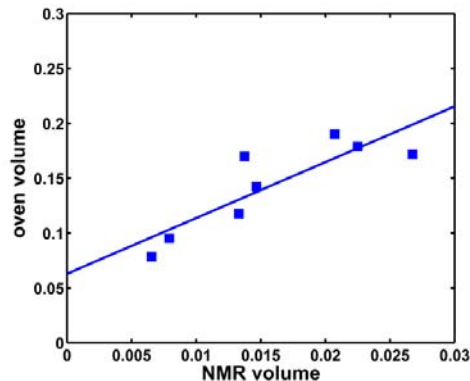
Figure 11: Comparison of mass lost via gravimetric methods and integration of T_1-T_2 NMR maps.

Caution must be used when directly comparing TGA and gravimetric results as such a comparison is highly dependent on factors such as heating rates, final temperatures, the time spent at each temperature and particle size. In the results presented here, the majority of mass change detected in the TGA-MS measurements corresponded to the cracking of solid hydrocarbons and the release of tightly bound water as well as chemical changes in the rock matrix while mass changes in our gravimetric results were dominated by the evolution of mobile water and hydrocarbons. In order to perform a more direct comparison to the two methods, efforts should be made to more closely match heating rates and temperature end points. Further work is currently underway to make such measurements.

CONCLUSION

This work was originally motivated by the observation of the dependence of T_1/T_2 as a function of TOC in shale A at 23 MHz relative to the response of the same material when measured at 2 MHz. The observed dependence of T_1/T_2 on frequency is predicted by theory, but an explanation for the dependence of T_1/T_2 on TOC is more difficult to model. It is, however, clear from the data that there is a relationship between these quantities. It is currently unclear what mechanism is responsible for the observed behavior. It is possible that the composition of the organic matter in the samples varies with depth and TOC and the variation in T_1/T_2 is simply a reflection of this change. Further work with a more fully characterized sample set will be necessary to attach a physical explanation to observations.

The weak dependence of T_2 on acquisition frequency is a useful addition to efforts to integrate downhole logging results with laboratory core analysis. We have shown that while acquisitions of T_1 and of T_1-T_2 maps can be strongly affected by frequency, measurements of the transverse relaxation time are not. This suggests that measuring T_2 at higher fields offers significantly shorter acquisition times with no additional uncertainty in the petrophysical quantities determined from such measurements.

Thermogravimetric analysis combined with mass spectroscopy allowed us to gain insight into composition of the pore fluids within our samples as well as the environment in which these fluids reside. We were able to demonstrate the ability to track relative changes in each type of fluid independently and correlate changes in the NMR response of our samples to changes in mass after baking at multiple temperatures. Ideally, the best fit line to this correlated data should pass through the origin, but assumptions regarding the relative amounts of water vs hydrocarbons as well as the hydrogen indices of the relevant pore fluids make a more definitive statement difficult at this point. More careful analysis of TGA-MS data on a more fully characterized sample set is needed. Neither sample set was preserved, and it is possible that an unknown amount of water could have evaporated before our experiments. Further thermal analysis will require better matching between the heating rates, times and temperature ranges of the TGA-MS process and oven drying as well as the use of preserved core material.

Finally, recent results in the literature suggest strongly that relaxation measurements at multiple NMR frequencies are critical to fully understand the physics of the water and hydrocarbons present in organic shales. We intend to perform nuclear magnetic dispersion measurements on preserved set of samples in the as-received state as well as after baking at the important temperatures determined by TGA-MS analysis.

ACKNOWLEDGEMENTS

REFERENCES
1. Odusina, E., & Sigal, R. F. (2011, February 1). Laboratory NMR Measurements on Methane Saturated Barnett Shale Samples. Society of Petrophysicists and Well-Log Analysts.
2. Rylander, E. Singer P.M., Jiang, T., Lewis, R., McLin, R., Sinclair, S., (2013, April 10). NMR T2 Distributions in the Eagle Ford Shale: Reflections on Pore Size. Society of Petroleum Engineers. doi:10.2118/164554-MS
3. Washburn, K. E., & Birdwell, J. E. (2013, August 12). A New Laboratory Approach to Shale Analysis Using NMR Relaxometry. Society of Petroleum Engineers. doi:10.1190/URTEC2013-181
4. Washburn, K.E., Birdwell, J.E., Seymour, J.D., Kirkland, C., Vogt, S.J. *Proc. Soc. Core Anal.* **2013**, SCA2013-002
5. Washburn, K.E., Birdwell, J.E., Updated methodology for nuclear magnetic resonance characterization of shales, J. Magn. Reson. **233**, 17-28 (2013)
6. Fleury, M. *Proc. Soc. Core Anal.* **2014** SCA2014-014
7. Washburn, K. E. (2014), Relaxation mechanisms and shales. Concepts Magn. Reson., 43A: 57–78. doi: 10.1002/cmr.a.21302
8. Daigle, H., Johnson, A., Gips, J. P., & Sharma, M. (2014, August 28). Porosity Evaluation of Shales Using NMR Secular Relaxation. Society of Petroleum Engineers. doi:10.15530/urtec-2014-1905272

9. Marc Fleury, Maria Romero-Sarmiento, Characterization of shales using T_1-T_2 NMR maps, Journal of Petroleum Science and Engineering, Volume 137, January 2016, Pages 55-62, ISSN 0920-4105

10. Kausik, R., Minh, C.C., Zielinksi, L., Vissapragada, B., Akkurt, R., Song, Y., Liu, C., Jones, S., Blair, E., (2011, January 1). Characterization of Gas Dynamics in Kerogen Nanopores by NMR. Society of Petroleum Engineers. doi:10.2118/147198-MS

11. Kleinberg, R.L., Farooqui, S.A., T_1/T_2 Ratio and Frequency Dependence of NMR Relaxation in Porous Sedimentary Rocks, Journal of Colloid and Interface Science **158**, 195-198 (1993)

12. Ozen, A. E., & Sigal, R. F. (2013, February 1). T1/T2 NMR Surface Relaxation Ratio for Hydrocarbons and Brines in Contact with Mature Organic-Shale Reservoir Rocks. Society of Petrophysicists and Well-Log Analysts.

13. Dynamics and Wettability of Oil and Water in Oil Shales, Jean-Pierre Korb, Benjamin Nicot, A. Louis-Joseph, Salvatore Bubici, and Gianni Ferrante, The Journal of Physical Chemistry C 2014 118 (40), 23212-23218

14. J-P Korb 2011 *New J. Phys.* **13** 035016

15. Nicot B, Vorapalawut N, Rousseau B, Madariaga LF, Hamon G, Korb J-P. 2015. Estimating Saturations in Organic Shales Using 2D NMR. SCA2015-024, Society of Core Analysts Symposium, St. John's, Newfoundland and Labrador, Canada.

16. Zhang, B., & Chen, J. (2014, August 28). Characterization of Shale Oil Rocks Using Retort and NMR. Society of Petroleum Engineers. doi:10.15530/urtec-2014-1922466

17. Gips, J., Daigle, H., & Sharma, M. (2014, August 28). Characterization of Free and Bound Fluids in Hydrocarbon Bearing Shales Using NMR and Py-GC-MS. Society of Petroleum Engineers. doi:10.15530/urtec-2014-1917686

18. Multivariate Analysis Relating Oil Shale Geochemical Properties to NMR Relaxometry, Justin E. Birdwell and Kathryn E. Washburn, Energy & Fuels 2015 29 (4), 2234-2243

19. Etherington, J. R., & McDonald, I. R. (2004, January 1). Is Bitumen a Petroleum Reserve? Society of Petroleum Engineers. doi:10.2118/90242-MS

20. Bloembergen, N., Purcell, E.M., Pound, R.V., Relaxation Effects in Nuclear Magnetic Resonance Absorption, Phys. Rev. **73**, 679 (1948)

21. Abragam, A., 1961, Principles of Nuclear Magnetism

22. http://www.mathworks.com/matlabcentral/fileexchange/37388-fast-2d-peak-finder

23. Handwerger, D.A., Keller, J., Vaughn, K., Improved Petrophysical Core Measurements on Tight Shale Reservoirs Using Retort and Crushed Samples, SPE (2011), 147456

24. Handwerger, D.A., Willberg, D., Pagels, M., Rowland, B., Keller, J.F., Reconciling Retort versus Dean Stark Measurements on Tight Shales, SPE (2012), 159976